JOURNAL OF STRUCTURAL BIOLOGY **117,** 16–23 (1996)
ARTICLE NO. 0065

A Triclinic Crystal Form of the Lectin Concanavalin A

PANAGIOTIS N. KANELLOPOULOS AND PAUL A. TUCKER[1]

European Molecular Biology Laboratory, D-69012 Heidelberg, Germany

AND

KYRIAKI PAVLOU, BOGOS AGIANIAN, AND STAVROS J. HAMODRAKAS

Departement of Biochemistry, Cell and Molecular Biology and Genetics, University of Athens, Panepistimiopolis, Athens 157 01, Greece

Received January 23, 1996, and in revised form April 8, 1996

The molecular structure of a triclinic crystal form of concanavalin A has been refined at 2.4 Å resolution. The crystals have unit cell dimensions a = 78.8 Å, b = 79.3 Å, c = 133.3 Å, α = 97.1°, β = 90.2°, and γ = 97.5° and contain two tetramers per asymmetric unit each with approximate 222 symmetry. The final crystallographic R-factor is 0.205 and the free-R-factor is 0.265 in the resolution range 6.0 to 2.4 Å. The conformation of the tetramer is more similar to that found in concanavalin A saccharide complexes than in the previously reported I222 crystal form of uncomplexed concanavalin A. A comparison of the molecular packing between the two crystal forms shows a more open arrangement with large solvent channels through the crystal.

INTRODUCTION

Plant lectins are a class of proteins of biological and medical interest because they serve as invaluable tools in the field of cell recognition and are found in a wide range of organisms (Lis and Sharon, 1986; Sharon and Lis, 1989a,b). They show a high degree of sequence similarity, suggesting similarity of function although the functional details remain unclear (for a review see Goldstein and Poretz, 1986).

The largest family of plant lectins is the Leguminosae lectins (van Driesshe, 1988; Reeke and Becker, 1988; Sharon and Lis, 1990). The best known member of the family is concanavalin A (ConA), which was isolated from the Jack bean (*Canavalia ensiformis*) and crystallized 6 decades ago (Sumner and Howell, 1936). ConA binds specifically to carbohydrates possessing the α-D-mannose or α-D-glucose group but also shows some affinity for other saccharide residues. Its carbohydrate binding properties make ConA a model protein in biological and biochemical research (Bittiger and Schnebli, 1976). ConA has a variety of biological activities. It effects the mobility of cell surface receptors (Yahara and Edelman, 1972, 1973), is a T-cell mitogen (Andersson *et al.*, 1972), and agglutinates a variety of cell types (Inhar and Sachs, 1969).

In solution, at pH values above 7, ConA is a tetramer, while at pH values below 6, it is a dimer (Kalb and Lustig, 1968; McKenzie *et al.*, 1972). Each monomer is a 237-residue polypeptide which requires the presence of two divalent metal ions for saccharide binding (Goldstein and Poretz, 1986). The first site (S1) contains Mn^{2+} but can bind other transition metals, while the second (S2) binds Ca^{2+} with Cd^{2+} as the only alternative (Kalb and Levitzki, 1968; Yariv *et al.*, 1968).

The three-dimensional structure of ConA was initially determined in an I222 crystal form (Edelman *et al.*, 1972; Hardman and Ainsworth, 1972) and later refined independently by two groups (Becker *et al.*, 1976; Hardman *et al.*, 1982) and some errors were corrected (Weisgerber and Helliwell, 1993) at higher resolution. High-resolution structures with the same crystal packing have been reported with the S1 site occupied by Cd^{2+} (Naismith *et al.*, 1993), Ni^{2+} (Emmerich *et al.*, 1994), or Co^{2+} (Emmerich *et al.*, 1994). Different crystal packings are found for the apo enzyme (Shoham *et al.*, 1979) and not surprisingly, for structures with bound saccharide molecules (Derewenda *et al.*, 1989; Naismith *et al.*, 1994; Kanellopoulos *et al.*, 1996). In all structures the ConA is observed as a tetramer with approxi-

Atomic coordinates have been deposited with the Brookhaven Protein Data Bank as entry 1VLN.

[1] To whom correspondence should be addressed at Structural Biology (including Biocomputing) Programme, EMBL, Meyerhofstrasse 1, D69012 Heidelberg, Germany. Fax: (06221) 387306. Email tucker@EMBL-Heidelberg.de.

1047-8477/96 $18.00

mate 222 symmetry. Here we report the structure of ConA in a triclinic crystal form at 2.4 Å resolution.

MATERIALS AND METHODS

Concanavalin A was purified as described previously (Kanellopoulos *et al.,* 1996) to yield a protein solution containing 70 mg/ml of ConA, 20 m*M* Tris (pH 8.0), 20 m*M* $MnCl_2$, and 20 m*M* $CaCl_2$. Crystallization was by a batch method. To the protein solution a 10 m*M* Tris, pH 8.5, 1 *M* $(NH_4)_2SO_4$ buffer was added in a 1:1 ratio, at 4°C. The crystals are trapezoidal prisms, with maximum dimensions $1.0 \times 0.8 \times 0.8$ mm and grow over a period of 3 weeks. They are triclinic, space group P1 with unit cell dimensions a = 78.8 Å, b = 79.3 Å, c = 133.3 Å, $\alpha = 97.1°$, $\beta = 90.2°$, and $\gamma = 97.5°$, and two tetramers per asymmetric unit.

X-ray diffraction data from seven crystals were collected at room temperature, to 2.4 Å maximum resolution, on a 30-cm MAR Research image plate detector. Pyrollytic graphite monochromatised CuK_α radiation (λ = 1.5418 Å) was used, produced by a rotating anode generator running at 40 kV, 70 mA. The rotation method was employed and 1° oscillation data frames were collected. The X-ray data were processed using the program XDS (Kabsch, 1988). A summary of the data collection statistics is given in Table I. We attribute the high R-factor primarily to radiation damage during data collection. We have attempted flash cooling the crystals but have been unable to find appropriate conditions, at least in part because it would not be sensible to use sugars as cryoprotectants.

The structure was solved by molecular replacement, using a ConA tetramer derived from the 2.75-Å model of the ConA: 4-nitrophenyl-α-D-mannopyranoside complex (α-PNM, Kanellopoulos *et al.,* 1996). The saccharide and all water molecules were omitted from the initial search model. All rotational and translational searches were carried out with the program AMoRe (Navaza, 1994). Using the fast rotation function calculation, reflections in the resolution range 15 to 3.5 Å, and an integration radius of 45 Å, a set of four dominant peaks appeared. The highest of the four peaks was 16.6σ and the remaining three had slightly lower values. The set of the four peaks were approximately related by 222 symmetry. The first two peaks, related by an approximate twofold, were chosen. The translation function calculations were performed using reflections from 15 to 3.5 Å. One peak for each rotation function solution was identified in the translation function and the corresponding crystallographic R-factor was 0.367. The rigid body refinement procedure, implemented in AMoRe, was applied and gave, for two tetramers per asymmetric unit, an initial crystallographic R-factor of 0.360 for the resolution range 15–2.5 Å.

TABLE I
Summary of Data Collection

Resolution (Å)	R_{sym} (%)[a]	% ofreflections with $I > 3\sigma(I)$	% of unique reflections measured
50.0–10.0	6.6	76.1	82.8
10.0–6.0	8.9	88.4	91.1
6.0–4.5	9.9	90.3	92.5
4.5–3.8	12.8	89.4	93.9
3.8–3.2	18.9	81.3	95.0
3.2–2.8	40.0	58.9	95.0
2.8–2.5	63.5	34.9	94.8
2.5–2.4	79.9	22.0	94.0
Total	17.4		

Note. Resolution range (Å), 50.0–2.4. Observed reflections, 445458. Unique reflections measured, 116878.

[a] $R_{sym} = \Sigma_h \Sigma_i |F_i^2(h) - \langle F^2(h)\rangle| / \Sigma_h \Sigma_i F_i^2(h)$.

TABLE II
Summary of Refinement of Triclinic ConA

Stage	Resolution range (Å)	R-factor	R-free
Molecular replacement solution (AMoRe)	15.0–2.5	0.360	—
Rigid body refinement (XPLOR)	6.0–2.5	0.285	0.279
Refinement (XPLOR)	6.0–2.5	0.209	0.267
Addition of 32 water molecules and refinement (XPLOR)	6.0–2.4	0.205	0.265

The model was further refined using the program X-PLOR (Brunger, 1992a). During all stages of refinement and model building, the eight non-crystallographically related molecules in the asymmetric unit were treated independently. Initially the model was subjected to rigid body refinement. Each of the monomers was treated as a separate rigid group and the refinement was performed for all data between 6.0 and 2.5 Å. After this stage, $2F_o$-F_c and F_o-F_c electron density maps were calculated and the fit of the model to the electron density was checked. The model rebuilding and map inspection were performed using the program O (Jones *et al.,* 1991). The model was then subjected to further refinement with X-PLOR taking into account, in the topology and parameter files, the cis peptide (Ala207–Asp208) bond. No restraints were placed on metal–ligand distances and no charge was attributed to the metal ions. A refinement step comprised simulated annealing refinement from a starting temperature of 3000 K, 120 cycles of conjugate gradient minimization, 15 cycles of overall B-factor refinement, 20 cycles of restrained individual B-factor refinement, and, finally, a further 160 cycles of conjugate gradient minimization. No sigma cutoff was applied and 90% of the data in the resolution range 6.0 to 2.5 Å were used in the refinement. In order to cross-validate in reciprocal space, the free-R-value (Brunger, 1992b) was monitored during all steps of refinement using the remaining 10% of the data. The electron density was then recalculated and the model was readjusted in parts. A total of 32 water molecules in the region of the metal binding sites were added to the model. The final model was obtained after further refinement using data in the resolution range 6.0 to 2.4 Å and has a crystallographic R-factor of 0.205 and a free-R-factor of 0.265. The refinement statistics are shown in Table II. We note that the inclusion of data in the resolution shell 2.5 to 2.4 Å in the refinement reduces the free-R-factor by 0.2% despite an R-merge of nearly 80% in that shell.

RESULTS AND DISCUSSION

Accuracy and Quality of the Model

The basic topology of the ConA monomers is unchanged from previously reported ConA structures (e.g., Naismith *et al.,* 1994) and will not be discussed further. A representative portion of the final $2F_o$-F_c electron density map is shown in Fig. 1a. A $2F_o$-F_c map calculated with reflections in the resolution range 15.0 to 2.4 Å has per residue real space correlation coefficients greater than 0.75 except in the loop containing residues 117 to 124. The coefficients were calculated for complete residues as implemented in O (Jones *et al.,* 1991) and is similar

for equivalent regions of the eight independently refined subunits.

The structure has good stereochemistry with rms deviations from ideality of 0.01 Å for bond lengths, 1.7° for bond angles, and 27° for dihedral angles. The maximum expected error in atomic positions is estimated to be between 0.35 and 0.40 Å based on a Luzatti plot (Fig. 1b; Luzatti, 1952). Only Asn118 of subunit C lies outside allowed regions of the Ramachandran plot (as calculated with the program PROCHECK; Laskowski *et al.*, 1993) but the density in this region is poor. The pattern of temperature factors is consistent for main chain and side chain atoms in the same subunit and also between the different subunits. They are also consistent with the real space correlation coefficients. The electron density is poor for the loop 117–124 in all subunits. This loop lies in the center of the hole formed by the ConA tetramer and is close to the region where the unusual posttranslational modification, which involves a ligation at residues 118 and 119, occurs (Bowles, 1990).

Description of the Structure

There are two tetramers in the asymmetric unit, the first is composed of subunits A through D and the second of subunits E through H (Fig. 2). The two tetramers have similar, but not identical, orientations relative to the unit cell axes. The second is rotated approximately 15° about *b* relative to the first. The crystal structure can be considered to be composed of infinite layers of ConA tetramers with relatively few contacts between the layers. The layers are approximately in the *ab* plane with alternating layers, along the *c* axis, composed of tetramers ABCD and EFGH. The interaction between tetramers along the crystallographic *a* axis is between subunits C and D and along the crystallographic *b* axis between subunits A and B. One layer of ABCD tetramers is shown in Fig. 3. The AB interface contains the hydrogen bonds HisA205 (NE2)-TyrB100 (OH) (2.6 Å) and SerA204 (OH) -ArgB228 (NH2) (3.0 Å) but otherwise the AB interface contacts are Van der Waals in nature with, presumably, additional solvent mediated contacts. The interactions primarily involve the loops 11–14, 18–23, 201–207, and 201–207 of molecule A with the loops 97–102, 201–207, 11–14, and 97–102 of molecule B, respectively. The CD interface has no short hydrogen bonds although the primary interactions are somewhat similar involving interactions between the loops 97–102, 97–102, and 201–207 of molecule C with the loops 11–14, 18–23, and 18–23 of molecule D, respectively. The contacts between molecules in the next layer are between G and H along *a* and between E and F along *b*. The EF contact is similar to the AB contact. It involves the same loops but the contacts are not identical in detail (e.g., HisE205(NE2)-TyrF100(OH) is 2.8 Å). In the same way the GH contact is similar but not identical to the EF contact. The packing of the layers along *c* is shown in detail in Fig. 4. It involves mainly two types of contacts, those between subunits A and G and those between D and F. The interaction between layers appears much better defined. It involves interactions between the loop containing residues 222–225 which projects from an otherwise flat protein surface. Thus, in the AG interface the hydrogen bonds AspA145(OD2)-SerG223(OG) (2.8 Å), GlyA224(N)-GlyG224(O) (2.8 Å), and SerA223(OG)-ThrG226(O) (2.5 Å) are observed. Similarily the DF interface shows the contacts AspF145(OD2)-SerD223(OG) (2.8 Å), GlyA224(N)-GlyG224(O) (2.8 Å), and SerF223(OG)-ThrD226(O) (2.7 Å).

The packing contrasts with the packing of concanavalin A molecules in the I222 crystal form. Very approximately, in the triclinic crystal form, if one considers the tetramer to be a tetrahedron the contacts between tetramers are at the apices of the tetrahedra, whereas in the I222 crystal form the apex of one tetrahedron interacts with the face of an adjacent tetrahedron. Probably because of the resulting larger interaction surface, there are more hydrogen bonding contacts between tetramers in the I222 crystal form (Weisgerber and Helliwell, 1993).

Superposition of the two tetramers in the asymmetric unit, calculated using the program O (Jones *et al.*, 1991), shows an rms difference of 0.46 Å for the 948 C^{α} atoms which is not much larger than the mean coordinate error estimated from the Luzatti plot (Fig. 1b). Superposition of the two tetramers with the tetramer found in the saccharide complexes of ConA with 4-nitrophenyl-α-D-mannopyranoside (Kanellopoulos *et al.*, 1996, α-PNM) and α-D-methylmannopyranoside (Naismith *et al.*, 1994; PDB entry: 5CNA) show similarily small deviations (ABCD/α-PNM 0.66 Å, EFGH/α-PNM 0.52 Å, ABCD/5CNA, 0.52 Å, and EFGH/5CNA 0.58 Å). Superposition of the ConA tetramers with that in the I222 crystal form (PDB entry: 2CTV), however, shows much larger rms differences (ABCD/2CTV 1.13 Å and DEFG/2CTV 1.30 Å). The superposition is shown in Fig. 5 for the ABCD tetramer. Qualitatively, the change is a movement about the center of mass of the tetramer of the A and B subunits toward each other. The C and D subunits also move toward each other, and consequently approximate 222 symmetry is retained. The loop 117–124 shows the largest change although, as mentioned above, this region exhibits poor electron density, presumably because, having no strong packing constraints, it is flexible. The central β-sandwich of the tetramer is essentially

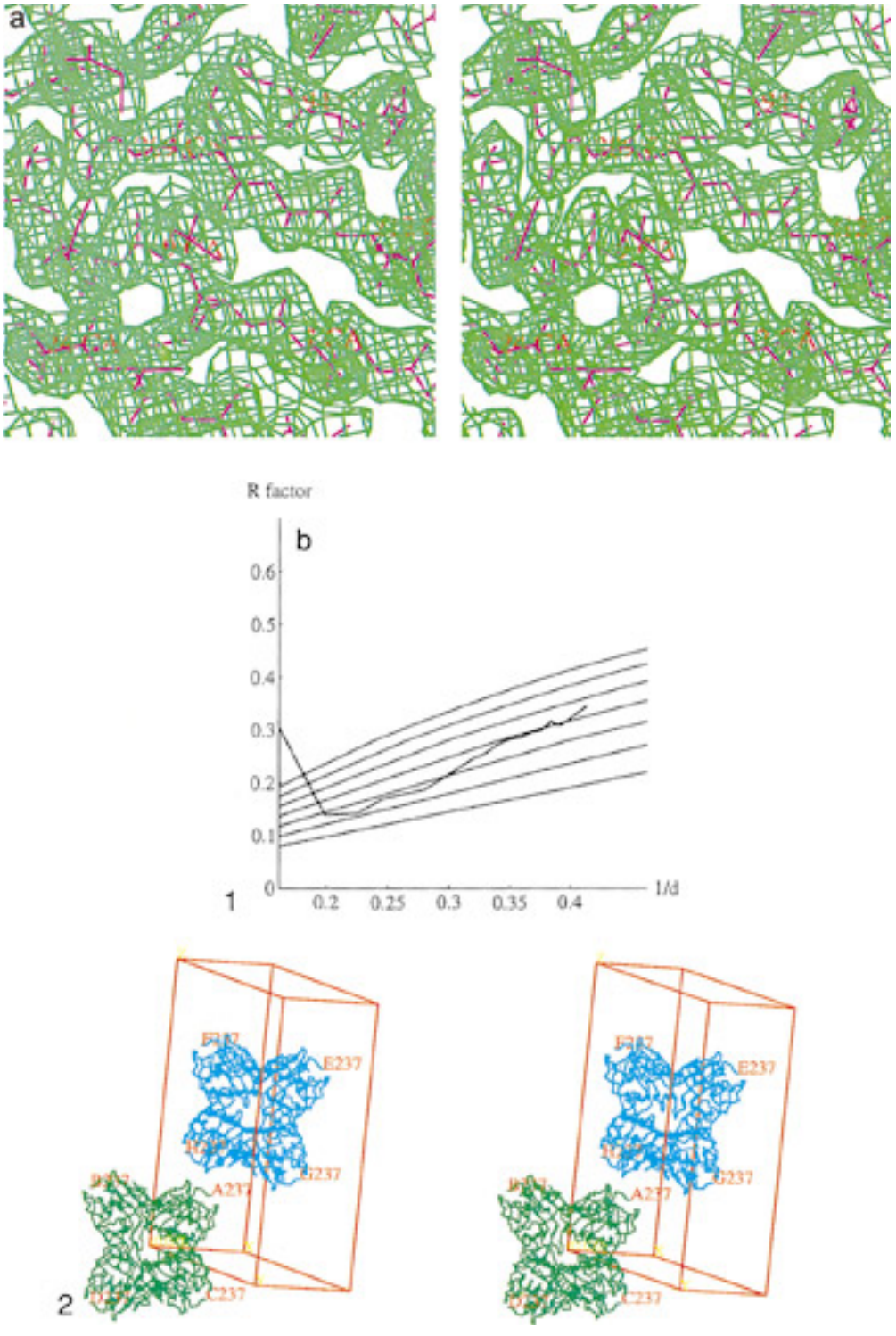

FIG. 1. (a) A stereo pair showing the final $2F_o$-F_c electron density in a β-strand region. The contouring is at 1.5 times the rms of the map. (b) The R-factor as a function of resolution together with theoretical curves based, from the bottom up, on coordinate errors of 0.2, 0.25, 0.3, 0.35, 0.4, 0.45, 0.5 Å, respectively.

FIG. 2. A stereo pair showing a C^{α} trace of the two molecules in the asymmetric unit. The tertramer composed of subunits A, B, C, and D is colored green and that composed of subunits E, F, G, and H is colored cyan. The C-termini of the polypeptide chains of each subunit are labeled.

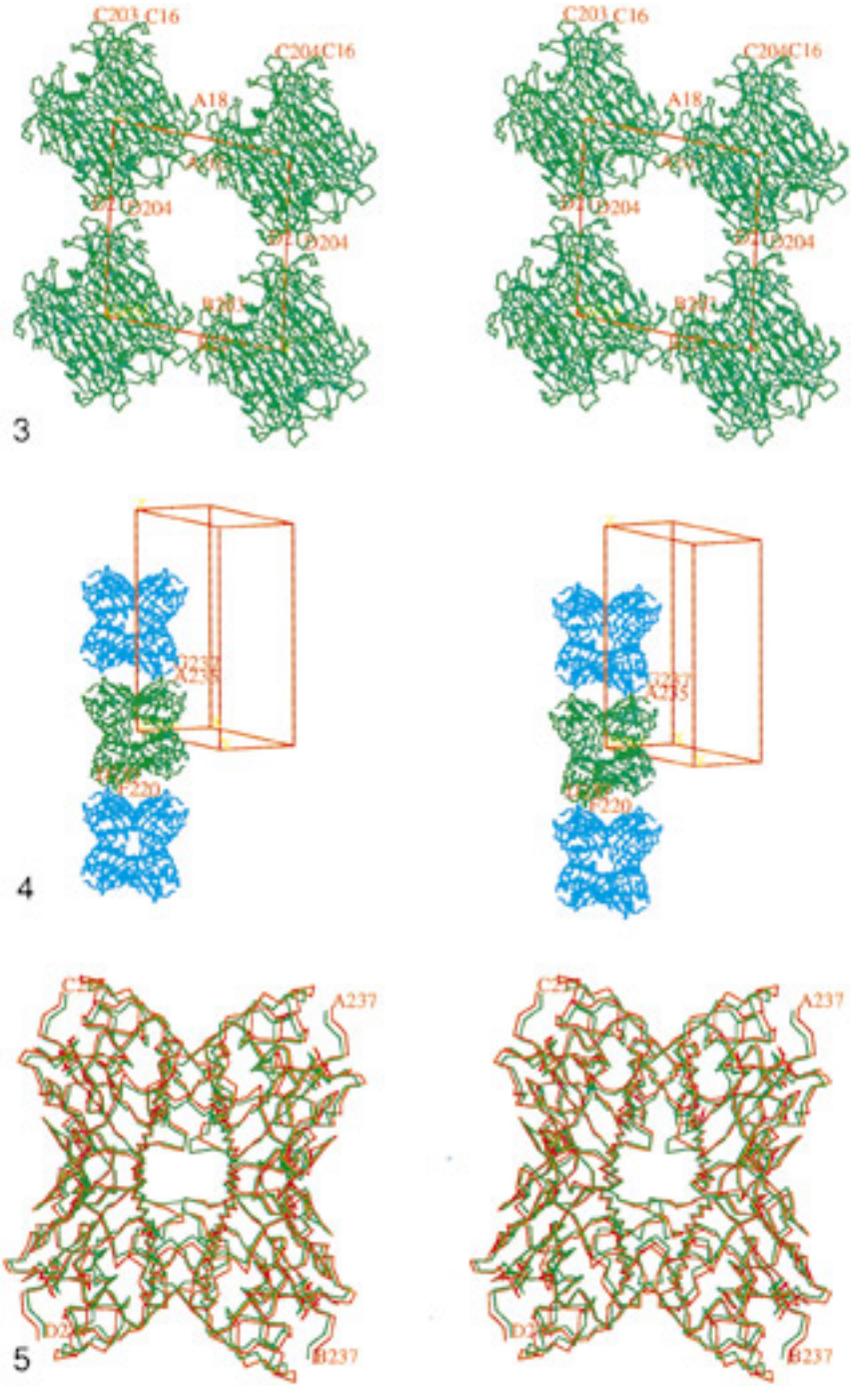

FIG. 3. A stereo pair showing the packing of ABCD tetramers in the crystallographic *ab* plane. Residues in loops primarily responsible for molecule–molecule contacts are labeled. The packing of the EFGH tetramers in the *ab* plane is similar, but not identical.

FIG. 4. A stereo pair showing the packing of ABCD tetramers (green) and EFGH tetramers (cyan) along the crystallographic *c* axis. Residues in loops primarily responsible for molecule–molecule contacts are labeled. The crystal is composed of alternate layers of cyan and green tetramers.

FIG. 5. A stereo pair showing the C^{α} superposition of the ConA tetramer ABCD in the triclinic crystal form (red) with the tetramer observed in the I222 crystal form (PDB code 2CTV, green). The EFGH tetramer is very similar to the ABCD tetramer.

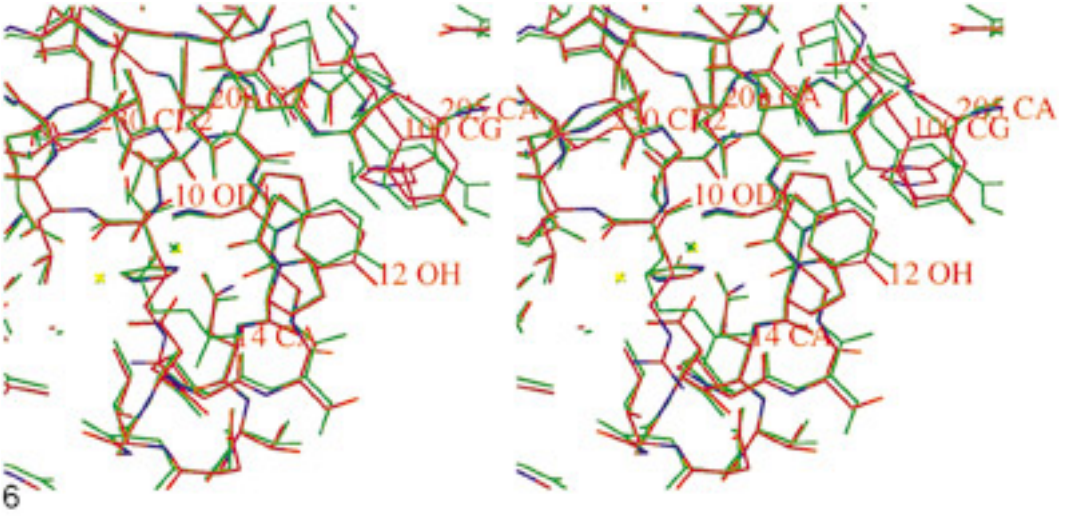

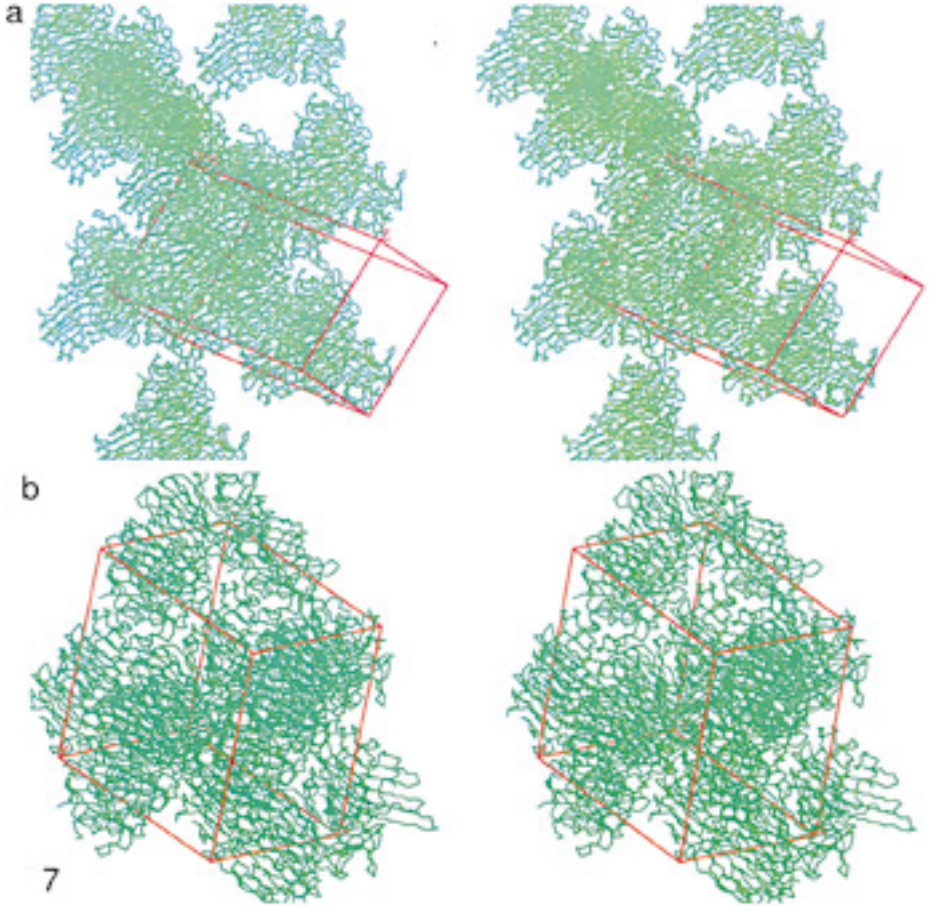

FIG. 6. A stereo pair showing the superposition of the saccharide binding sites of the ConA tetramer ABCD in the triclinic crystal form (colored by atom, with carbon (brown), oxygen (red), and nitrogen (blue) with that in the I222 crystal form (green). The atoms superimposed (using the program "O") were the C^{α} atoms of residues 7 to 36, 205 to 210, and 226 to 230.

FIG. 7. Stereo pairs showing the packing of ConA tetramers in the (a) triclinic and (b) I222 (PDB code 2CTV) crystal forms. The view in each case is chosen looking approximately perpendicular to the plane defined by the centres of mass of three subunits of the tetramer.

unchanged. The saccharide binding site (Fig. 6), which contains no significant electron density that can be interpreted in terms of a sugar molecule, is essentially identical in the two crystal forms. Figure 6 shows that there are differences in the side chain orientation of some surface residues close to, but not part of, the binding site.

The primary determinants for production of the triclinic crystal form seem to be lower temperature crystal growth (4°C) and a different buffering system when compared with conditions used to obtain the I222 crystal form. We cannot say why this might affect the intermolecular contacts and give rise to a different crystal packing, but it is worth observing that the ConA tetramer in this triclinic crystal form is more similar to that in all the saccharide complex structures reported to date than to that in the I222 crystal form. It is not possible on the basis of these data to decide whether the packing is determined by a lower energy conformation of the tetramer or whether the packing determines the conformation of the tetramer, but the former seems more likely because the packing is different for different saccharide complexes yet the molecular conformation is similar (the rms difference in C^{α} positions between α-PNM/5CNA is 0.64 Å).

As described above, the ConA tetramer, with approximate 222 symmetry and tetrahedral shape, forms networks of molecules which contact via the tips of the tetrahedra. These tips also contain the sugar binding site and it is tempting to speculate that agglutination is facilitated because the sugar binding sites are fairly evenly distributed over 4π steradians resulting in the maximum possible distance between them which in turn more readily allows binding to membrane bound saccharides from different cells. Tetramer–tetramer interactions, as observed in the crystal structures, may also aid the process of agglutination, generating attractive forces, albeit weak ones, between ConA tetramers. The crystal packing is of itself interesting because it is very open. There are solvent channels around 40 Å in diameter along *z*, with channels around 30 Å along the *x* and *y* axes. The solvent content is 72% compared with 54% in the I222 crystal form which has a solvent channel of around 25 Å in diameter along *z* only. A comparison of the packing of tetramers is shown in Fig. 7. The prospect of soaking crystals of the triclinic form of ConA with suitably sized molecules that are otherwise difficult to crystallize offers possibilities that we aim to explore further.

S.J.H. thanks the Supercomputing Resource for Molecular Biology (SRMB), funded by the European Union "Access to Large Scale Installations" Programme, for support.

REFERENCES

Andersson, J., Edelman, G. M., Moller, G., and Sjoberg, O. (1972) Activation of B lymphocytes by locally concentrated concanavalin A, *Eur. J. Immunol.* **2,** 233–235.

Becker, J. W., Reeke, G. N., Jr., Cunningham, B. A., and Edelman, G. M. (1976) New evidence on the location of the saccharide-binding site of concanavalin A, *Nature (London)* **259,** 406–409.

Bittiger, H. S., and Schnebli, H. P. (1976) Concanavalin A as a Tool, Wiley–Interscience, London.

Brunger, A. T. (1992a) X-PLOR Version 3.1: A System for X-ray Crystallography and NMR, Yale Univ., New Haven, CT.

Brunger, A. T. (1992b) Free R value: A novel statistical quantity for assessing the accuracy of crystal structures, *Nature* **335,** 472–475.

Derewenda, Z., Yariv, J., Helliwell, J. R., Kalb (Gilboa), A. J., Dodson, E. J., Papiz, M. Z., Wan, T., and Cambell, J. W. (1989) The structure of the saccharide-binding site of concanavalin A, *EMBO J.* **8,** 2189–2193.

Edelman, G. M., Cunningham, B. A., Reeke, G. N., Becker, J. W., Waxdal, M. J., and Wang, J. L. (1972) The covalent and three-dimensional structure of concanavalin A, *Proc. Natl. Acad. Sci. USA* **69,** 2580–2584.

Emmerich, C., Helliwell, J. R., Redshaw, M., Naismith, J. H., Harrop, S. J., Raftery, J., Kalb(Gilboa), A. J., Yariv, J., Dauter, Z., and Wilson, K. S. (1994) High-resolution structures of single-metal-substituted concanavalin A: The Co, Ca-protein at 1.6 Å and the Ni, Ca-protein at 2.0 Å, *Acta Crystallogr.* **D50,** 749–756.

Goldstein, I. J., and Poretz, R. P. (1986) *in* Liener, I. E., Sharon, N., and Goldstein, I. J. (Eds.), The Lectins: Properties, Functions and Applications in Biology and Medicine, pp. 33–247, Academic Press, New York.

Hardman, K. D., and Ainsworth, C. F. (1972) Structure of concanavalin A at 2.4-Å resolution, *Biochemistry,* **11,** 4910–4919.

Hardman, K. D., Agarwal, R. C., and Freiser, M. J. (1982) Manganese and calcium binding sites of concanavalin A, *J. Mol. Biol.* **157,** 69–86.

Imhar, M., and Sachs, L. (1969) The interaction of the carbohydrate-binding protein concanavalin A with normal and transformed cells, *Proc. Nat. Acad. Sci. USA* **63,** 1418–1425.

Jones, T. A., Zou, J. Y., Cowan, S. W., and Kjeldgaard, M. (1991) Improved methods for building protein models in electron density maps and the location of errors in these models, *Acta Crystallogr.* **A47,** 110–119.

Kabsch, W. (1988) Evaluation of single-crystal X-ray diffraction data from a position-sensitive detector, *J. Appl. Crystallogr.* **21,** 916–924.

Kalb, A. J., and Lustig, A. (1968) The molecular weight of concanavalin A, *Biochim. Biophys. Acta* **168,** 366–367.

Kalb, A. J., and Levitzki, A. (1968) Metal-binding sites of concanavalin A and their role in the binding of α-methyl-D-glucopyranoside, *Biochem. J.* **109,** 669–672.

Kanellopoulos, P. N., Pavlou, K., Perrakis, A., Agianian, B., Vorgias, C. E., Mavrommatis, C., Soufi, M., Tucker, P. A., and Hamodrakas, S. J. (1996) The crystal structure of the complexes of concanavalin A with 4′-nitrophenyl-α-D-mannopyranoside and 4′-nitrophenyl-α-D-glucopyranoside, *J. Struct. Biol.*, **116,** 345–355.

Laskowski, R. A., MacArthur, M. W., Moss, D., and Thornton, J. M. (1993) PROCHECK: A program to check the stereochemical quality of protein structures, *J. Appl. Crystallogr.* **26,** 283–291.

Lis, H., and Sharon, N. (1986) *in* Liener, I. E., Sharon, N., and Goldstein, I. J. (Eds.), The Lectins: Properties, Functions and Applications in Biology and Medicine, pp. 265–291, Academic Press, New York.

Luzatti, V. (1952) Traitement statistique des erreurs dans la determination des structures cristallines, *Acta Crystallogr.* **5,** 802–810.

McKenzie, G. H., Sawyer, W. H., and Nichol, L. W. (1972) The molecular weight and stability of concanavalin A, *Biochim. Biophys. Acta* **263,** 283–293.

Naismith, J. H., Habash, J., Harrop, S. J., Helliwell, J. R., Hunter, W. N., Wan, T. C. M., Weisgerber, S., Kalb(Gilboa), A. J., and Yariv, J. (1993) Refined structure of cadmium-substituted concanavalin A at 2.0 Å resolution, *Acta Crystallogr.* **D49,** 561–571.

Naismith, J. H., Emmerich, C., Habash, J., Harrop, S. J., Helliwell, J. R., Hunter, W. N., Raftery, J., Kalb(Gilboa), A. J., and Yariv, J. (1994) Refined structure of concanavalin A complexed with methyl-a-D-mannopyranoside at 2.0 Å resolution and comparison with the saccharide-free structure, *Acta Crystallogr.* **D50,** 847–858.

Navaza, J. (1994) AMoRe: An automated package for molecular replacement, *Acta Crystallogr.* **A50,** 157–163.

Reeke, G. N., Jr., and Becker, J. W. (1988) Carbohydrate-binding sites of plant lectins, *Curr. Topics Microbiol. Immunol.* **139,** 35–58.

Sharon, N., and Lis, H. (1989a) Lectins, Chapman & Hall, London.

Sharon, N., and Lis, H. (1989b) Lectins as cell recognition molecules, *Science* **246,** 227–234.

Sharon, N., and Lis, H. (1990) Legume lectins—A large family of homologous proteins, *FASEB J.* **4,** 3198–3208.

Shoham, M., Yonath, A., Sussman, J. L., Moult, J., Traub, W., and Kalb, A. J. (1979) Crystal structure of demetallized concanavalin A: The metal-binding region, *J. Mol. Biol.* **131,** 137–155.

Sumner, J. B., and Howell, S. F. (1936) The identification of the haemagglutinin of Jack bean with concanavalin A, *J. Bacteriol.* **32,** 227–237.

Weisgerber, S., and Helliwell, J. R. (1993) High-resolution crystallographic studies of native concanavalin A using rapid Laue data collection methods and the introduction of a monochromatic large-angle oscillation technique (LOT), *J. Chem. Soc. Faraday Trans.* **89,** 2667–2675.

Van Driessche, E. (1988) Structure and funtion of leguminosae lectins, *in* Franz, H. (Ed.), Advances in Lectin Research, Vol. 1, pp. 73–134, Springer-Verlag, Berlin.

Yahara, I., and Edelman, G. M. (1972) Restriction of the mobility of lymphocyte immunoglobulin receptors by concanavalin A, *Proc. Nat. Acad. Sci. USA* **69,** 608–612.

Yahara, I., and Edelman, G. M. (1973) The effects of concanavalin A on the mobility of lymphocyte surface receptors, *Exp. Cell Res.* **81,** 143–155.

Yariv, J., Kalb, A. J., and Levitzki, A. (1968) The interaction of concanavalin A with methyl-α-D-glucopyranoside, *Biochim. Biophys. Acta* **165,** 303–305.